Photo-oxidative action in MCF-7 cancer cells induced by hydrophobic cyanines loaded in biodegradable microemulsion-templated nanocapsules

KAZIMIERA A. WILK[1], KATARZYNA ZIELIŃSKA[1], JADWIGA PIETKIEWICZ[2], NINA SKOŁUCKA[2], ANNA CHOROMAŃSKA[2], JOANNA ROSSOWSKA[3], ARNOLD GARBIEC[4] and JOLANTA SACZKO[2]

[1]Department of Chemistry, Wroclaw University of Technology, Wybrzeże Wyspiańskiego 27, 50-370 Wroclaw;
[2]Department of Medical Biochemistry, Medical University of Wroclaw, Chałubińskiego 10, 50-368 Wroclaw;
[3]Institute of Immunology and Experimental Therapy Polish Academy of Sciences, Rudolfa Weigla 12, 53-114 Wroclaw;
[4]Department of Animal Developmental Biology, University of Wroclaw, Sienkiewicza 21, 50-355 Wroclaw, Poland

Received October 7, 2011; Accepted December 19, 2011

DOI: 10.3892/ijo.2012.1458

Abstract. Searching for photodynamic therapy-effective nanocarriers which enable a photosensitizer to be selectively delivered to tumor cells with enhanced bioavailability and diminished dark cytotoxicity is of current interest. We have employed a polymer-based nanoparticle approach to encapsulate the cyanine-type photosensitizer IR-780 in poly(*n*-butyl cyanoacrylate) (PBCA) nanocapsules. The latter were fabricated by interfacial polymerization in oil-in-water (o/w) microemulsions formed by dicephalic and gemini saccharide-derived surfactants. Nanocarriers were characterized by SEM, AFM and DLS. The efficiency of PBCA nanocapsules as a potential system of photosensitizer delivery to human breast cancer cells was established by dark and photocytotoxicity as the function of the cellular mitochondria. The photodynamic effect of cyanine IR-780 was determined by investigation of oxidative stress markers. The nanocapsules were the main focus of our studies to examine their cellular uptake and dark and photocytotoxicity as the function of the cellular mitochondria as well as oxidative stress markers (i.e., lipid peroxidation and protein damage) in MCF-7/WT cancer cells. The effects of encapsulated IR-780 were compared with those of native photosensitizer. The penetration of the nanocapsules into cancer cells was visualized by CLSM and their uptake was estimated by FACS analysis. Cyanine IR-780 delivered in PBCA nanocapsules to MCF-7/WT cells retains its sensitivity upon photoirradiation and it is regularly distributed in the cell cytoplasm. The intensity of the photosensitizer-generated oxidative stress depends on IR-780 release from the effective uptake of polymeric nanocapsules and seems to remain dependent upon the surfactant structure in o/w microemulsion-based templates applied to nanocapsule fabrication.

Correspondence to: Dr Jolanta Saczko, Department of Medical Biochemistry, Medical University of Wroclaw, Chałubińskiego 10, 50-368 Wroclaw, Poland
E-mail: jolasak@gmail.com

Key words: nanocarriers, photodynamic therapy, cyanine, lipid peroxidation, oxidative protein damage

Introduction

Successful treatment of cancer depends on the effectiveness of cytotoxic anticancer therapies, either alone or in combination with other ways of treatment. Therefore, there is a need for new diagnostic and therapeutic techniques with significantly improved sensitivity and specificity. Photodynamic therapy (PDT) is a relatively new anticancer treatment which both offers an alternative approach to conventional methodologies and receives quite noticeable acceptance in oncology (1,2). In contrast to chemo- and radiation therapies PDT provides fewer adverse side effects and higher selectivity. Its dominant mechanism of action comprises overproduction of reactive oxygen species (ROS), inducing oxidative stress in malignant cells. ROS react with lipids and thiol groups of proteins, and cause damage to cellular membranes. Among these targets, peroxidation of lipids is particularly damaging because the formation of lipid peroxidation products leads to a facile propagation of free radicals (3). PDT can induce cell death through necrosis or apoptosis dependent on the photosensitizer used, illumination conditions, oxygenation status of tissue and the type of cells involved (4). However, the intracellular localization of the sensitizer coincides with the primary site of photodamage (5). Numerous photosensitizers have been examined *in vitro* and *in vivo*, including porphyrins and chlorines, and a few of them have revealed ideal features for PDT (6). Furthermore, some groups of light-sensitive cyanine dyes were also identified as photosensitizers (7). The cyanine derivatives, a complex group of dyes containing numerous subgroups featuring cationic and anionic compounds, appear to have interesting properties and they have been studied as potential PDT dyes in recent years. Some authors have reported on application of indocyanine green, squarylium cyanine and MC540 in photodynamic therapy (8,9). Such structures were used for the selective

removal of ocular leukemia, lymphoma, and neuroblastoma cells (10). Although the cyanines appear interesting for PDT treatment, in clinical trials the same side effects were observed as the results of dark toxicity of photosensitizers towards cancer and normal cells (6). For this reason, the incorporation of such hydrophobic molecules into biocompatible nanocapsules may reduce cytotoxicity of a free photosensitizer and permit the delivery of greater amounts of such cargo to the cancer cells. In the literature there are many examples of polymeric nanoparticles designed as drug nanocarriers (11-13), including those which comprise nanocapsules consisting of a liquid core (mainly water) surrounded by a thin polymer envelope (14,15). Oil-containing nanocapsules were obtained mainly by the polymerization of alkyl cyanoacrylates at the oil/water interface of very fine o/w emulsions (16,17). In the literature some poly(alkyl cyanoacrylate) nanocapsules were found suitable for the delivery of a water-soluble bioactive compound, for example as potential nanocarriers for oligonucleotides (18), proteins (19), and peptide drugs (20,21).

We have previously reported on IR-768 cyanine molecules encapsulated in non-ionic microemulsion-templated nanocapsules, which being internalized in MCF-7 breast cancer cells, effectively enhance cell death after light irradiation (17,22). As a continuation of our search for new polymeric template-mediated nanoproducts we focused our present studies on the systematic evaluation of the template-type influence on the biological response of the given nanocarrier. For interfacial polymerization of *n*-butyl cyanoacrylate, four kinds of oil-in-water (o/w) microemulsions were employed as templates: those stabilized by biodegradable and biocompatible saccharide-derived surfactants of a dicephalic structure, i.e., N-dodecyl-N, N-bis[(3-D-glucoheptonylamido)propyl]amine (C12DGHA) and N-dodecyl-N,N-bis[(3-D-gluconylamido)propyl]amine (C12DGA) (23); and the gemini representatives N,N'-bisdodecyl-N,N'-bis[(3-glucoheptonylamido)propyl]ethylene diamine (bis(C12GHA)) and N,N'-bisdodecyl-N,N'-bis[(3-gluconylamido) propyl]ethylene diamine (bis(C12GA)) (structures are shown in Fig. 1) (24,25). Using different types of surfactant architectures to form o/w microemulsions offers the flexibility to choose the microemulsion template that provides optimal loading, release and biological impact in the cell environment. Accordingly, the aim of our study was to evaluate the cytotoxic effect and metabolic consequences of PDT realized by means of a so-called third generation photosynthesizer, i.e., a hydrophobic cyanine IR-780 (structure is shown in Fig. 1A) encapsulated in polymeric microemulsion-templated nanocapsules and delivered to cancer cells. The physical characteristics of obtained nanoproducts such as size distribution, apparent shape, microelectrophoretic behavior and colloidal stability were investigated by means of dynamic light scattering (DLS), Doppler laser electrophoresis, scanning electron microscopy (SEM) and atomic force microscopy (AFM). Biological examinations comprised examination of mitochondrial metabolic function and description of the main oxidative markers, i.e., lipid peroxidation and protein oxidative damage in relation to each template/surfactant/nanocapsule. The penetration of the nanocapsules into cancer cells was visualized by a confocal laser scanning microscope (CLSM) and cytofluorimetric analysis (FACS). Introduction and light excitation (λ 760-800 nm) of photosensitizer IR-780 to the MCF-7/WT cells was found to induce oxidative stress.

Materials and methods

Reagents. Photosensitizer IR-780 with the chemical structure as shown in Fig. 1A, diethylene glycol monoethyl ether (EMGD), ethanol, iso-butanol and Dulbecco's modified Eagle's medium (DMEM) were purchased from Sigma-Aldrich. *N*-butyl cyanoacrylate was kindly given to us by Tong Shen Ent. Co., (Taiwan). Surfactants, namely dicephalic N-dodecyl-N, N-bis[(3-D-glucoheptonylamido)propyl]amine (C12DGHA) and N-dodecyl-N,N-bis[(3-D-gluconylamido)propyl]amine (C12DGA), as well as gemini N,N'-bisdodecyl-N,N'-bis[(3-glucoheptonylamido)propyl]ethylenediamine (bis(C12GHA)) and N,N'-bisdodecyl-N,N'-bis[(3-gluconylamido)propyl] ethylenediamine (bis(C12GA)), were synthesized as previously described (23,25,26) (for structures see Fig. 1B and C). Water used in all the experiments was doubly distilled and purified by means of the Millipore Milli-Q purification system (Bedford, MA).

Preparation of microemulsion-templated nanocapsules with and without cyanine IR-780. Microemulsions were prepared as described previously (17). Briefly, oil-in-water microemulsions, containing 5% surfactant, 5% iso-butanol as a cosurfactant (at a 1:1 surfactant-to-cosurfactant weight ratio), 5% diethylene glycol monoethyl ether as an oil, and 85% water, were prepared by mixing appropriate amounts of all components in vials by shaking at ambient temperature. For the preparation of cyanine-loaded microemulsion, oil with the dissolved IR-780 powder was used as the oil component of the microemulsion. Nanoparticles were prepared based on the method described in ref. 17: 50 μl of *n*-butyl cyanoacrylate monomer was dissolved in 150 μl of chloroform and slowly added to 10 ml of the selected microemulsion template (empty or loaded with the photosensitizer IR-780). Interfacial polymerization was performed at 4˚C and the system was stirred for at least 4 h to complete the synthesis. The nanocapsules were collected by centrifugation at 10,000 rpm for 15 min at 25˚C (Eppendorf centrifuge, Unipen 310 rotor), washed several times with ethanol and dried. Entrapment of IR-780 (E %) was determined indirectly by measuring the concentration of the remaining cyanine in the supernatant following the isolation of the nanoparticles. The difference between the mass of cyanine solubilized in the polymerization template and the unloaded amount measured in the supernatant of the resulting nanocapsule dispersion following centrifugation was determined (Metertech SP8001 spectrophotometer with 1-cm-path-length thermostated quartz cell). All measurements were performed in triplicate. E (%) was calculated by E (%) = [(IR-780)tot - (IR-780) free)/(IR-780)]tot x 100.

Characterization of nanoparticle size, surface charge and morphology. The particle size and distribution of both the o/w microemulsions and the PBCA nanocapsules were determined by dynamic light scattering (DLS) (Zetananosizer Nano series ZS, Malvern Instruments Ltd.) according to directions given in ref. 27. The zeta potential of the poly(*n*-butyl cyanoacrylate) nanocapsules dispersed in 1 mM sodium chloride solution was determined by electrophoretic mobility using the Zetananosizer Nano series ZS instrument. The external structure of the dry nanocapsules was visualized by a scanning electron microscope (SEM) (Jeol, JSM-5800 LV), in which ethanol dispersions of the

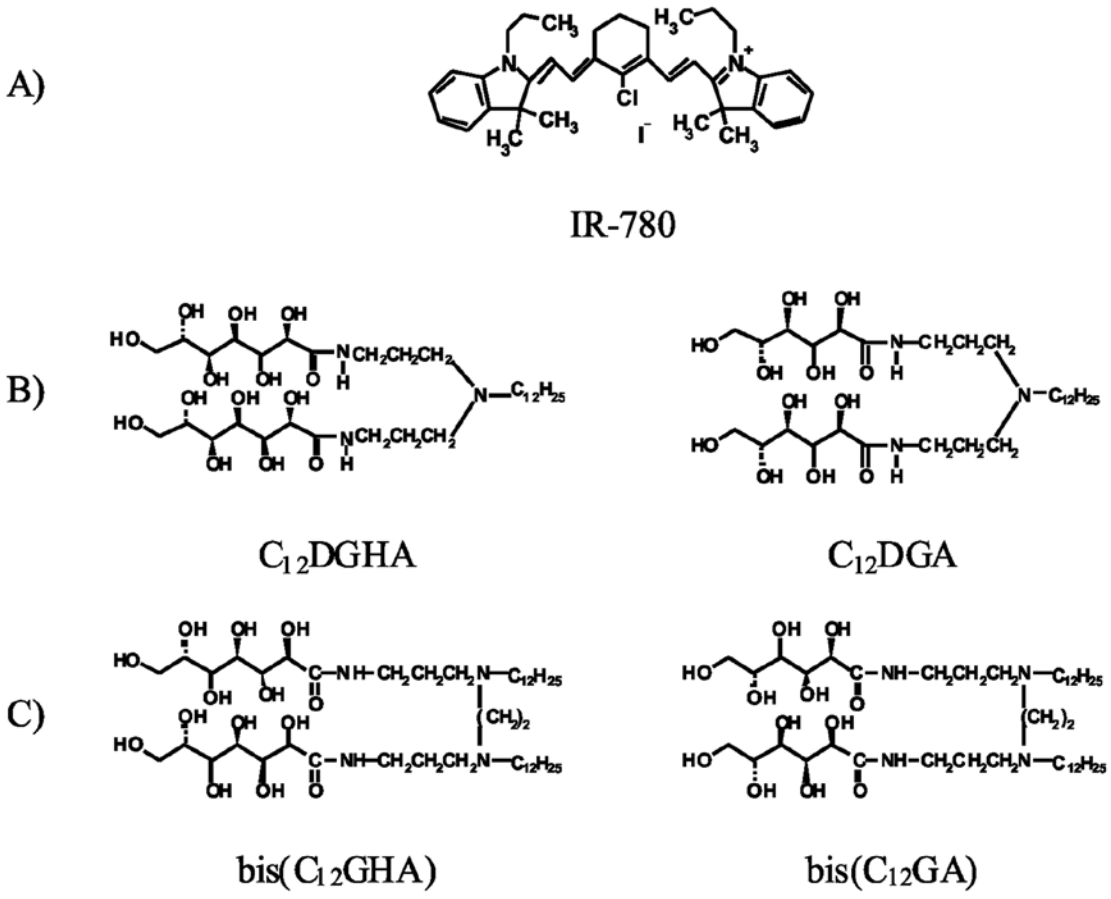

Figure 1. Compounds studied: (A) cyanine IR-780, (B) dicephalic and (C) gemini type of non-ionic aldonamide-type surfactants.

nanocapsules were placed on the sample holder, the ethanol was allowed to evaporate, and the nanocapsules were coated with carbon. The samples were viewed at an accelerating voltage of 22 kV. Atomic force microscopy (AFM) was performed as follows. A total of 20 μl of an ethanol suspension of the nanoparticles was deposited on a freshly cleaned mica surface, which corresponds to an approximate surface concentration of 10 molecules/μm^2. The samples were then dried overnight. Imaging was carried out using the ultra-low-amplitude tapping mode on a Veeco NanoScope Dimension V AFM with an RT ESP Veeco tube scanner. Scanning speeds were 0.5 Hz and a low-resonance-frequency pyramidal silicon cantilever resonating at 250-331 kHz was used (force constant: 20-80 N/m). The amplitude of the resonance was set manually to the lowest possible for stable imaging within the contamination layer present on the surface.

Cell culture. A well-characterized and photodynamically examined human malignant doxorubicin-sensitive cell line (MCF-7/WT) was used. The human breast adenocarcinoma cell line MCF-7 is derived from a pleural effusion taken from a 69-year-old Caucasian female with metastatic breast cancer. The cell line was a kind gift from the Department of Tumor Biology, Comprehensive Cancer Center, Maria Sklodowska-Curie Memorial Institute in Gliwice. The cell line was cultivated in the growth medium Dulbecco's modified Eagle's medium (DMEM, Sigma) supplemented with 10% fetal calf serum (Biowhittaker) and antibiotics (penicillin/streptomycin, Sigma) in 25 ml TC flasks (Falcon) at 37˚C, in a 5% CO_2 humidified atmosphere. For the experiments the cells were removed by trypsinization (trypsin 0.025% and EDTA 0.02%; Sigma) and washed with PBS.

Cytotoxicity studies after photoirradiation of MCF-7/WT cancer cells treated with free or encapsulated IR-780. The MTT assay (Sigma) was used to test the mitochondrial metabolic function of MCF-7/WT breast cancer cells. The experimental conditions were described in a previous report (17). Briefly, the cells were plated at a density of 2x10^5 cells in 0.2 ml of DMEM on 96-well plates and incubated at 37˚C in a 5% CO_2 atmosphere. After 24 h of culture, the medium in the plate was replaced with 0.2 ml of fresh DMEM. Thereafter, 50 μl aliquots of samples containing free cyanine IR-780 at a concentration range of 2-15x10^{-6} M or unloaded or IR-780-loaded nanocapsules were added to 0.2 ml of cell suspension in DMEM and the incubation was continued overnight. The IR-780 concentration in all experiments with loaded nanocapsules was adjusted to be the same as that of the free dye. Control cells (negative control without cyanine IR-780 or with empty nanocapsules) were processed in the same way. The conditions for cancer cell light irradiation were established according to previous reports (28,29). The cells were irradiated for 10 min with a total light dose of 6 J/cm^2 using a lamp (OPTEL Opole, Fibre Illuminator, Poland) with polarized light and a red filter (λ max 632.8 nm). The energy fluency rate was 10 mW/cm^2

at the level of the cell monolayer. The influence of nanocapsules unloaded and loaded with cyanine IR-780 as well as free cyanine on MCF-7/WT cell survival was assayed after 24-h incubation at 37˚C. The MTT test was then performed. The absorbance of the resulting solutions from three duplicate experiments was read at a wavelength of 570 nm in an ELISA microplate reader (Labsystems Multiscan MS, Finland). The calculated data were expressed as the percentage of cell survival.

Fluorescent activated cell scanning (FACS). Flow cytometric studies were performed for a quantitative study of intracellular uptake of PBCA nanocapsules loaded with IR-780 by the MCF-7/WT breast cancer cell population. The samples containing $3x10^5$ cells/ml were incubated for 24 h with cyanine-loaded nanocapsules following the previous reported procedure (17), under final cyanine IR-780 concentration of $15x10^{-6}$ M. The cells treated with comparative amounts of nanocapsule analogs without cyanine were a negative control. The positive control sample contained MCF-7/WT cells incubated with $15x10^{-6}$ M free cyanine. Intracellular IR-780 fluorescence detection was carried out using a FACSCalibur flow cytometer (Becton-Dickinson) equipped with argon laser (488 nm) and red diode (633 nm). After excitation of cell samples at 633 nm, the fluorescence of IR-780 was measured by an FL-4 detector. Data were analyzed using CellQuest software (Becton-Dickinson) and presented as histograms as well as the geometric mean (GMean) fluorescent emission intensities of positive cells (30,31).

Confocal laser scanning microscopy (CLMS) method of cyanine IR-780 localization in MCF-7/WT cells treated with PBCA nanocapsules loaded with photosensitizer molecules. To localize the cyanine IR-780 in the cell monolayer by CLSM, microcultures of MCF-7/WT cells were trypsinized from the culture flasks and harvested on cover glasses in Petri dishes for 24 h. Then free cyanine IR-780 diluted in DMEM was added to reach a final concentration of $15x10^{-6}$ M and an equivalent concentration of IR-780 contained in PBCA nanocapsules based on the templates C_{12}DGA:*iso*-butanol/EMGD/water, C_{12}DGHA:*iso*-butanol/EMGD/water, bis(C_{12}GHA):*iso*-butanol/EMGD/water and bis(C_{12}GA):*iso*-butanol/EMGD/water was delivered as well. The cells were incubated for 24 h at 37˚C, fixed with 4% paraformaldehyde, and washed with PBS. The slides were then mounted on the stage of a CLSM Olympus FluoView FV1000 confocal laser scanning microscope (Olympus). The fluorescent emission of cyanine IR-780 delivered to the cells was determined after excitation at 405 nm. The images (512x512 pixels) were recorded by employing a Plan-Apochromat 63x oil-immersion objective (NA: 1.4). An HFT 405/488/561 dichroic mirror and an LP 575 emission filter were used in channel 2 for detecting photosensitizer emission. Each fluorescent image was colored in red and represented an optical slice with a thickness of 1 μm. Transmitted light images were acquired simultaneously.

Oxidative stress markers. The MCF-7/WT cells were treated with nanocapsules loaded with IR-780 at equivalent $10x10^{-6}$ M cyanine concentration. Control samples contained nanocapsules without cyanine. The cells were incubated for 24 h at 37˚C and irradiated for photooxidative stress stimulation. The total light dose of 6 J/cm^2 was emitted for 10 min using a lamp (OPTEL Opole, Fibre Illuminator) with polarized light and a red filter (λ max 632.8 nm). The energy fluency rate was 10 mW/cm^2 at the level of the cell monolayer. Incubation of MCF-7/WT was continued for 3 h and 6 h and then cells were removed by trypsinization and resuspended in PBS.

Lipid peroxidation. The final product of cellular fatty-acid peroxidation, malondialdehyde (MDA), was determined according to earlier studies (29,32). The MDA reacts with thiobarbituric acid (TBA) to form a colored complex, TBARS, whose level was measured by the absorbance at a wavelength of 535 nm. The concentration of MDA was quantified spectrophotometrically based on a set of MDA standards of known concentration.

Protein damage. Photooxidative stress induces a decrease of the level of free-SH groups in cellular proteins. Accordingly, the protein damage was estimated by the modified Ellman's method in which DTNB acid reacted with thiol groups (-SH) of proteins. The level of -SH groups was measured spectrophotometrically on the basis of the absorbance at the wavelength of 412 nm (29).

Statistical analysis. Unless otherwise indicated, all the data are mean values ± SD calculated from at least three independent experiments. Student's t-test was used to test for the significance level between independent variables. The level of significance was set at $p<0.05$.

Results and Discussion

The focus of this study was to prepare and characterize photosensitizer IR-780 loaded poly(*n*-butyl cyanoacrylate) nanocapsules (PBCA nanocapsules) with the goal of enhancing its bioavailability without loss of biological activity. These nanoparticles were examined for their cellular uptake, and for their ability to induce cyto- and photocytotoxicity as well as to generate oxidative stress in the MCF-7/WT cancer cells. Throughout the studies, the effects of encapsulated IR-780 were compared with those of native photosensitizer.

Properties of empty and IR-780 loaded microemulsion-templated nanocapsules. Nanoparticles were prepared by interfacial polymerization of *n*-butyl cyanoacrylate in four selected microemulsions (characteristic features are provided in Table I) stabilized with different aldonamide-type surfactants. When the oil component of the microemulsion was replaced by cyanine dye dissolved in diethylene glycol monoethyl ether (EMGD), no change in phase behavior of the system was evident. This could be due to a stabilizing effect from the sugar-based surfactants, as reported in ref. 20. The diameter of the obtained nanocapsules was dependent on the template type (Table II). Accordingly, the nanocapsule size ranged from 224 to 264 nm for unloaded nanocapsules and from 233 to 276 nm for nanocarriers with encapsulated photosensitizer. The low and moderate values of the polydispersity index (PdI) determined for most of the microemulsions are in the range of 0.08-0.10 (Table I) and for obtained IR-loaded nanocapsules 0.10-0.13 (Table II) and characterize a reasonable monodispersity of the systems (33). All IR-780 loaded nanoparticles had a negative zeta potential ranging from -27.9 to -32.1.

Table I. Physicochemical properties of microemulsion templates.

	Microemulsion (surfactant:*iso*-butanol/EMGD/water)							
	Surfactant		Content (wt %)					
Abbreviation	HLB[a]	CMC[b] (mM)	Concentration (mM)	Surfactant: cosurfactant (1:1)	EMGD[c]	Water	D_H[d] (nm)	PdI[e]
C_{12}DGHA	13.4	0.316	69	5	5	85	3.9	0.102
bis(C_{12}GHA)	7.9	0.0052	53	5	5	85	4.8	0.097
C_{12}DGA	11.8	0.251	76	5	5	85	3.5	0.085
bis(C_{12}GA)	6.3	0.0038	57	5	5	85	4.2	0.082

[a]HLB, hydrophilic liophilic balance; [b]CMC, critical micellar concentration (23,24); [c]EMGD, diethylene glycol monoethyl ether; [d]D_H, hydrodynamic diameter; [e]PdI, polydispersity index.

Table II. Characteristics of empty and IR-780-loaded poly(*n*-butyl cyanoacrylate) nanocapsules.

		Nanocapsules						
		Empty			Loaded with IR-780			
No.	Microemulsion/template	D_H[a] (nm)	PdI[b]	ξ[c] (mV)	D_H[a] (nm)	PdI[b]	ξ[c] (mV)	E %[d]
1	C_{12}DGHA:*iso*-butanol/EMGD/water	241	0.13	-29.5	233	0.10	-29.6	92
2	bis(C_{12}GHA):*iso*-butanol/EMGD/water	224	0.15	-31.2	234	0.12	-31.0	92
3	C_{12}DGA:*iso*-butanol/EMGD/water	264	0.20	-27.7	276	0.13	-27.9	90
4	bis(C_{12}GA):*iso*-butanol/EMGD/water	246	0.21	-32.5	244	0.13	-32.1	90

[a]D_H, hydrodynamic diameter; [b]PdI, polydispersity index; [c]ξ zeta potential; [d]E%, entrapment efficiency.

The morphologies of the nanoparticles were found to be spherical with a smooth surface and no change was apparent upon loading with photosensitizer (Fig. 2). The encapsulation efficiency was around 90% and was slightly dependent on the microemulsion template used for polymerization. As can be observed, there is no significant difference in size or zeta potential value between empty and IR-780-loaded nanocapsules, indicating that these active molecules were associated with the oily core of the microemulsions rather than adsorbed on their surface.

Dark toxicity and photodynamic effect. Photodynamic therapy activates a new generation of photosensitizers belonging to the cyanine family by illumination with visible light (>630 nm), generating photocytotoxic effects (34,35). Here we present the results of a preliminary study to investigate therapeutic effects of active cyanine IR-780 delivered by new synthesized polymeric nanocapsules to a human cancer cell line. The viability of MCF-7/WT cells as the function of the cellular mitochondria was measured by MTT assay after 24-h incubation with both free and encapsulated cyanine. The results related to the dark toxicity evaluation of empty and IR-780 loaded PBCA nanocapsules are presented in Fig. 3. There is no noticeable effect of empty nanocapsules on viability of MCF-7/WT cells, which indicates that the studied cyanine-free nanocarriers do not change the metabolic conditions of the breast cancer cells. Morever, a cell survival decrease after MCF-7/WT incubation with IR-780 nanocarriers resulted from the cyanine dark toxicity only when high doses of nanocapsules were used. We have previously observed a similar effect of polymeric nanocapsules fabricated by means of classical non-ionics comprising unloaded and loaded cyanine IR-768 products (17).

The cytotoxicity of unirradiated nanocarriers with IR-780 increased along with the increase of cyanine concentration in the examined samples (Fig. 3). However, nanocapsule 1 (systems according to Table II) based on a template stabilized with dicephalic glucoheptonyl surfactant C12DGHA caused a noticably higher decrease of MCF-7/WT cell viability in comparison to nanocapsule 2 containing the template which was stabilized by gemini glucoheptonyl surfactant bis(C12GHA). Nanocarrier systems 3 and 4 loaded with IR-780 caused diminished dark cytotoxicity (Fig. 3B) in comparison to those mentioned above.

The irradiation process of cells treated with IR-780 loaded nanocarrier 1 was found to induce quite a significant photodynamic effect in comparison to system 2 (Fig. 4A). Moreover, photocytotoxicity of nanocapsules 3 and 4 (Fig. 4B) was lower than that of 1 and 2. Such findings may suggest that the observed differences in the cyanine cyto- as well as photocytotoxicity result in varied delivery efficiency of IR-780 to the MCF-7/WT cells, which seems to be directly determined by the template type,

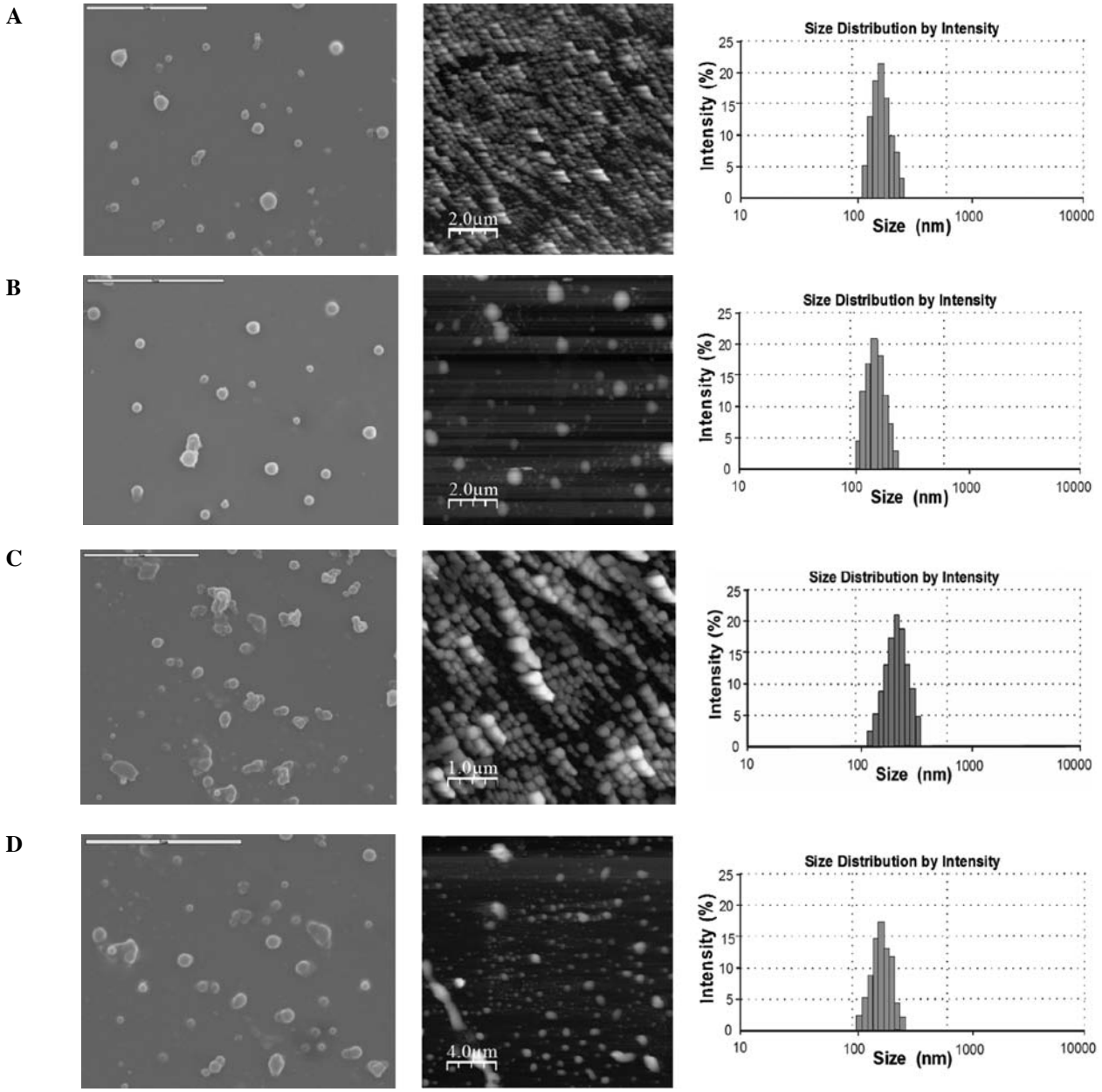

Figure 2. IR-780 loaded nanocapsule morphology by scanning electron microscopy (SEM), atomic force microscopy (AFM) and size by dynamic light scattering (DLS) for particles obtained from: (A) C_{12}DGA:*iso*-butanol/EMGD/water, (B) C_{12}DGHA:*iso*-butanol/EMGD/water; (C) bis(C_{12}GHA):*iso*-butanol/EMGD/water and (D) bis(C_{12}GA):*iso*-butanol/EMGD/water microemulsion templates.

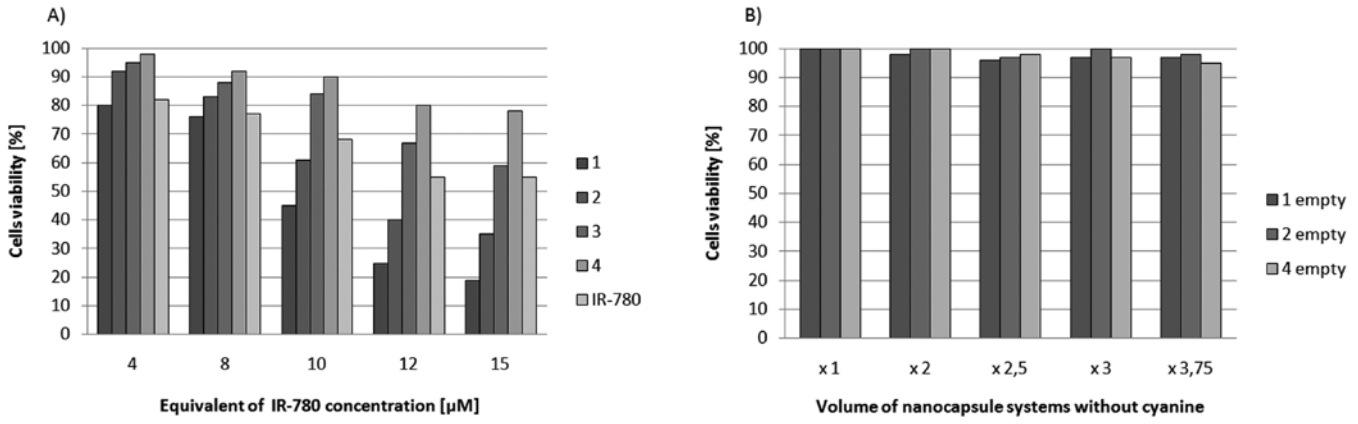

Figure 3. The effect of free and encapsulated IR-780 cyanine on the viability of MCF-7/WT cells before irradiation: dye-loading nanocapsule systems 1-2 (A) and 3-4 (B), according to Table I and their analogues without cyanine (empty 1, 2 and 4).

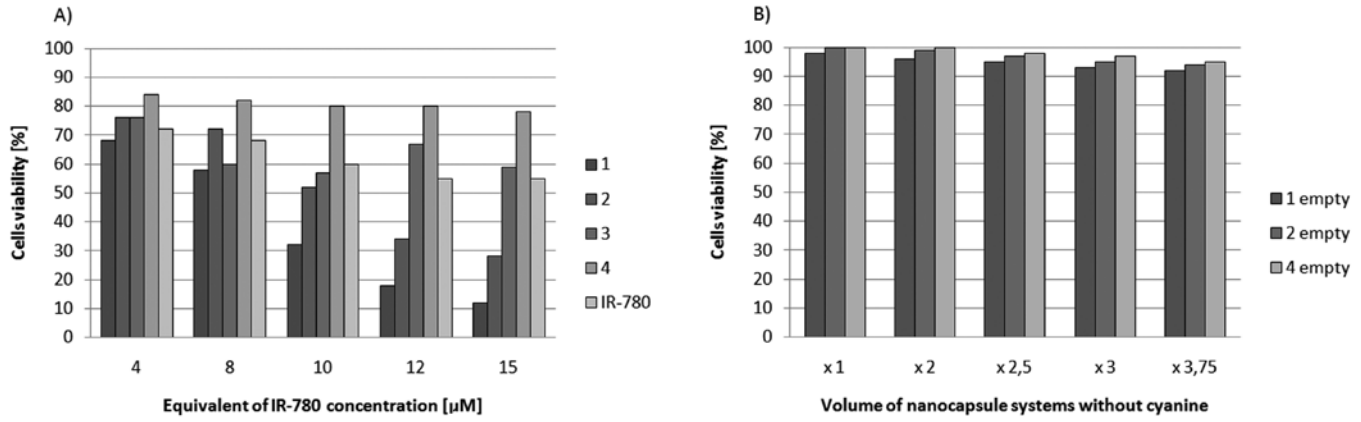

Figure 4. The effect of free and encapsulated IR-780 cyanine on the viability of MCF-7/WT cells after irradiation: dye-loading nanocapsule systems 1-2 (A) and 3-4 (B), according to Table I and their analogues without cyanine (empty 1, 2 and 4).

i.e., the surfactants' different structural architecture (dicephalic vs. gemini) and their hydrophobic-hydrophilic parameters such as hydrophilic-lipophilic balance (HLB) (Fig. 1 and Table I). We have recently reported that hemolytic activity of a variety of aldonamide-type surfactants against human erythrocytes (36) and cytotoxicity in MCF-7/WT cells of saccharide-based microemulsions (37) are of a noticeable level, especially when C12DGA is considered. The cytotoxic and photocytotoxic properties of PBCA nanocapsules based on microemulsion templates of the dicephalic type gluconyl surfactant (system 3 according to Table II, stabilized by C12DGA) or the gemini derivative [system 4 according to Table II, stabilized by bis(C12GA)] are in accordance with the observation that system 3 is more effective as a cyanine nanocarrier. However, somewhat better results were achieved for nanocapsules fabricated by means of the glucoheptonyl surfactants [i.e., C12DGHA or bis(C12GHA)].

According to the literature data the cellular uptake of nanocarriers by endocytosis and endosome/lysosome formation determines the release mechanism of the therapeutic agent to the cytoplasm and other cellular organelles (38,39). There are possibilities that the structure of non-ionic sugar surfactants changes the lysosome lipid membrane stability in different ways. When the nanocapsule internalization by the treated cells proceeds by the endocytosis mechanism, one can assume that their more hydrophobic components being released in the lysosomes will solubilize the hydrophobic IR-780 to a higher extent. Furthermore, the phospholipid bilayer of the lysosome membrane will be more stabilized. We can suppose that the hydrophobic photosensitizer penetration from the lysosome to the cell cytoplasm and eventually to the mitochondrion will proceed with more difficulty than for the cargo encapsulated in nanocapsules fabricated from more hydrophilic surfactants (Table II). The verification of this hypothesis is in progress.

FACS fluorescence detection of cyanine IR-780 delivered with polymeric nanocapsules to the human breast cancer cells. Our present findings propose PBCA nanocapsules as a convenient carrier for the hydrophobic cyanine IR-780. In this study, the cellular association and internalization of IR-780-loaded PBCA nanocapsules were assessed in flow cytometry, which facilitated the exploration of cellular compartmentalization without cell lysis, a method commonly used in other studies (40,41). The *in vitro* IR-780 accumulation in MCF-7/WT cells has been examined after their incubation with the PBCA nanocapsules based on o/w microemulsion templates consisting of the following pseudoternary systems: C_{12}DGA:*iso*-butanol/EMGD/water, C_{12}DGHA:*iso*-butanol/EMGD/water, bis(C_{12}GHA):*iso*-butanol/EMGD/water, bis(C_{12}GA):*iso*-butanol/EMGD/water. The final concentration of cyanine was $15x10^{-6}$ M in all experiments. The FACS analysis showed cellular uptake of IR-780 cyanine delivered in various nanocapsule systems and permitted the quantification of photosensitizer delivery in the total population of examined cancer cells as the geometric mean of fluorescence emission intensity (Fig. 5). The GMean fluorescence signal emission intensity of IR-780 transported with nanocapsules containing microemulsion templates C_{12}DGHA:*iso*-butanol/EMGD/water (GMean 217.44) or bis(C_{12}GHA):*iso*-butanol/EMGD/water (GMean 103.44) was significantly higher than autofluorescence of untreated cancer cells (GMean 3.84) as well as the signal emitted by the empty nanocarriers - GMean 4.59 (Fig. 5A and B vs. G and F, respectively. It is worth noting that the obtained histograms prove good metabolic conditions of MCF-7/WT cells in FACS experiments. The obtained nanocapsules effectively deliver IR-780 to the MCF-7/WT cells, in spite of the fact that the uptake of free photosensitizer is higher (GMean 309.27), as shown in Fig. 5E. The cell internalization of nanocapsules based on C_{12}DGA:*iso*-butanol/EMGD/water or bis(C_{12}GA):*iso*-butanol/EMGD/water templates is not very efficient (Fig. 5C and D), for the weak IR-780 fluorescence (GMean 6.74 and 4.59, respectively). Relative cell fluorescence determined as GMean of treated cells compared to negative control GMean is in Fig. 5H. The FACS analysis results correspond well with the observed effects in the cytotoxicity experiments (Fig. 3).

The efficiency of cyanine IR-780 delivery with various PBCA nanocapsules based on microemulsion C_{12}DGHA:*iso*-butanol/EMGD/water as the template was more efficient than that of nanocapsules containing bis(C_{12}GHA):*iso*-butanol/EMGD/water template, which was observed as a different right shift of histograms (Fig. 6). Probably, C12DGHA can better facilitate the cyanine release to the cell cytoplasm by changing the stability of endosomal vesicle membranes, as found by others (38,39).

Moreover, the FACS analysis was used for nanocapsule time-dependent stability determination. Our results indicate that

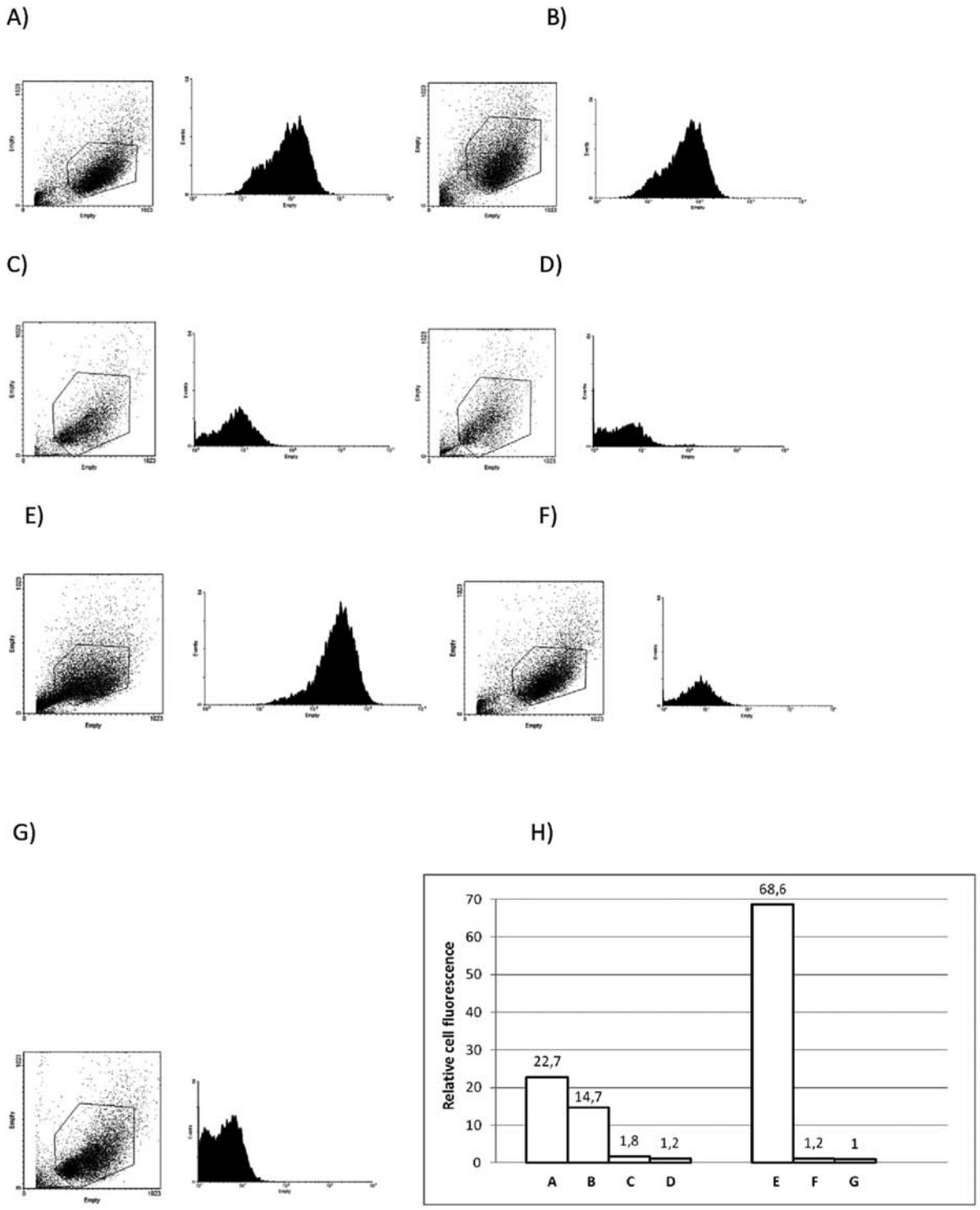

Figure 5. The FACS analysis of cyanine IR-780 fluorescence after delivery with polymeric nanocapsules to the MCF-7/WT cells. (A-G) Histograms of loaded cyanine IR-780 PBCA nanocapsules based on microemulsion templates: (A) C_{12}DGHA:*iso*-butanol/EMGD/water, (B) bis(C_{12}GHA):*iso*-butanol/EMGD/water, (C) C_{12}DGA:*iso*-butanol/EMGD/water, (D) bis(C_{12}GA):*iso*-butanol/EMGD/water. In control experiments, MCF-7/WT cells were incubated with: (E) free cyanine IR-780 (positive control), (F) unloaded nanocapsules of (A) system. Negative control contained not treated MCF-7/WT (G). (H) Relative fluorescence of investigated cells (A-G) experiments; GMean fluorescence intensity of untreated MCF-7/WT cells from (G) sample was considered as 1.

the nanocapsule dispersions in water stored at room temperature in dark conditions demonstrated good stability for over three months (Table III). We should also note that IR-780 loaded nanocapsules stored under the same conditions do not influence the MCF-7/WT autofluorescence even after quite a long time. However, as reported by Yordanov *et al*, a small decrease in the delivery efficiency of the loaded polymeric nanocapsules may be a consequence of partial erosion of PBCA nanocapsules (42). Additionally, some differences in uptake may be related to a discrepancy in divisional state of the cells or be caused by cell heterogeneity of the used tumor cell lines (43,44). Further studies are needed to clarify this problem.

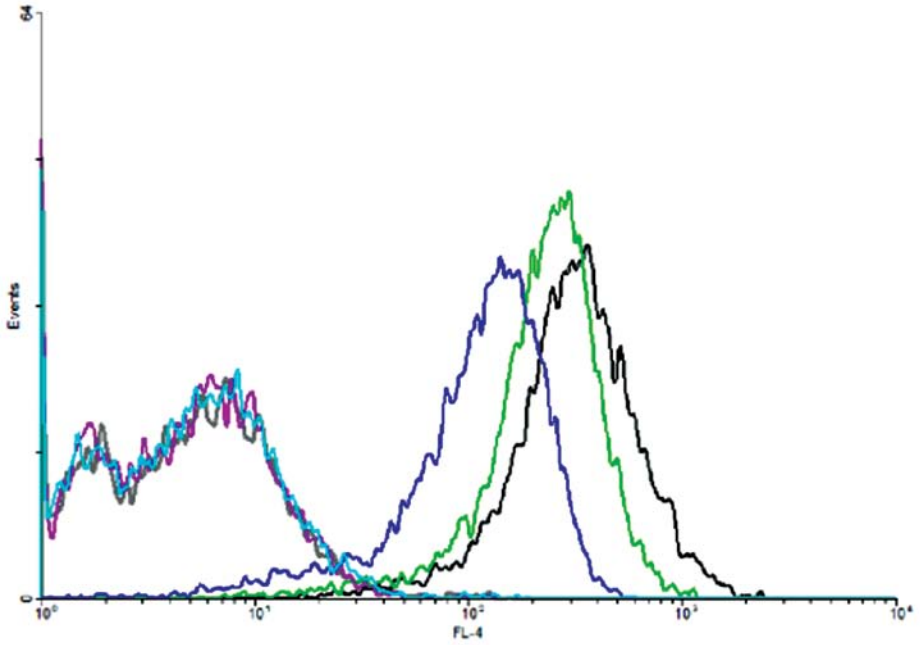

Figure 6. Flow cytometry analysis of MCF-7/WT cancer cells treated with IR-780 loaded PBCA nanocapsules. Diagram represents the GMean intensity signal of IR-780 delivered to the MCF-7/WT cells as free photosensitizer or encapsulated in nanocapsules based on C_{12}DGHA:*iso*-butanol/EMGD/water or bis(C_{12}GHA):*iso*-butanol/EMGD/water templates (black, green and navy blue line, respectively). Control samples with not treated MCF-7/WT cells or cells incubated with unloaded nanocupsules are decripted as gray, violet and blue line, respectively.

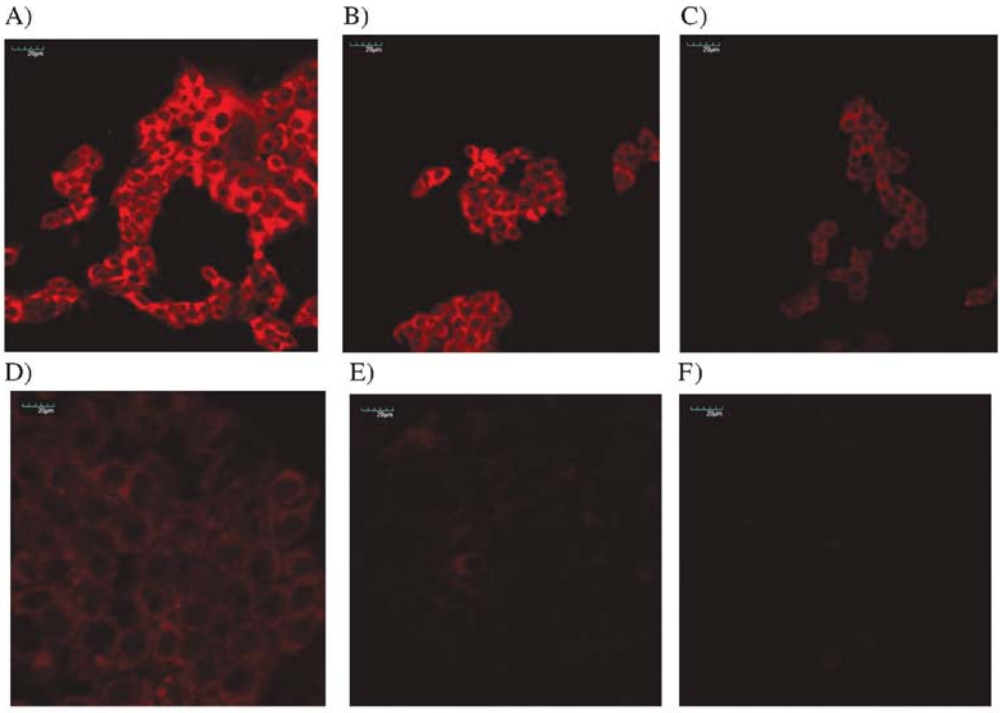

Figure 7. The cyanine IR-780 fluorescence emission in human breast cancer MCF-7/WT cells. Confocal microsope images of cells after 24-h incubation with (A) free cyanine or IR-780-loaded nanacapsules based on C_{12}DGHA:*iso*-butanol/EMGD/water or bis(C_{12}GHA):*iso*-butanol/EMGD/water templates (B and C, respectively). (D and E) system (B) and (C) after 15 weeks storage at room temperature and dark conditions. (F) Control cells not treated with nanocapsules. Scale bar, 20 μm.

Localization of IR-780 delivered with nanocapsules to the MCF-7/WT cells by CLMS. The localization of the cyanine IR-780 in the MCF-7/WT cells treated with free photosensitizer or IR-780-loaded nanocapsules was also examined in a confocal laser scanning microscope. The final 15 μM concentrations of IR-780 were used for the CLSM experiments due to the photobleaching phenomenon (45). The intracellular fluorescence emission after the excitation of cyanine IR-780 at 633 nm was observed as shown in Fig. 7. The photosensitizer molecules were regularly diffused in the cell cytoplasm and were not observed

Table III. Influence of nanocapsules storage time on the effectivity of IR-780 delivery by PBCA nanocapsules to the MCF-7/WT cells.

	Relative fluorescence emission of IR-780[a]			
			System	
Storage time (weeks)	1	2	1 empty	2 empty
1	30.0	22.7	1.0	1.0
5	21.4	14.0	1.0	1.0
10	9.4	6.3	1.0	1.0
15	8.5	4.0	1.0	1.0

Data for 10,000 cells in 0.5 ml sample analysed in cytofluorimeter. [a]Relative signal determined as the mean intensity of fluorescence emission obtained for cells incubated with nanocapsules related to autofluorescence of control cells not treated.

in the nucleus. Similar results of cyanine IR-768 or chemotherapeutic agent doxorubicin localization in MCF-7/WT cells was described previously for polymeric nanocapsules based on microemulsions stabilized by non-ionic commercial surfactants or for polyelectrolyte shells loaded with doxorubicin (17,46).

The empty nanocapsules do not show fluorescence emission in every case in control experiments (Fig. 7F), which indicates that the nanocapsules without cyanine do not stimulate the breast cancer cell autofluorescence. The cell morphology is normal, which corresponds with histograms of the FACS analysis, where only an insignificant amount of the cell population is dead (Fig. 5). Those results were confirmed by the MTT experiments (Fig. 3). Moreover, we can suggest that the studied dye essentially does not aggregate inside the cells and is able, therefore, to act as an efficient photosensitizer. Additionally, the intracellular localization of IR-780 indicates the usefulness of nanocapsules based on C_{12}DGHA:*iso*-butanol/EMGD/water or bis(C_{12}GHA):*iso*-butanol/EMGD/water templates, as nanocarriers for photosensitizer delivery, as was reported for other polymeric nanocapsules containing templates stabilized by non-ionic polyoxyethylene surfactants (17). Somewhat diminished fluorescence intensity of IR-780 in MCF-7/WT cells which were incubated with nanocapsules and stored for 15 weeks confirms the slight decrease of the efficiency of photosensitizer delivery observed also in the FACS analysis.

Oxidative stress markers. Most of the previous reports described only the cyto- and photocytotoxic effects of photosensitizers delivered to the cells with various nanocarriers (17,47). We first showed that the active photodynamic response leads to effective generation of oxidative stress in the MCF-7/WT cells treated with cyanine IR-780 containing the new type of polymeric nanocapsules. The ability to produce singlet oxygen and other reactive oxygen species depends on the aggregation state of photosensitizer molecules and the photobleaching effect (31,48). The incubation of MCF-7/WT cells with $10x10^{-6}$ M equivalent concentration of encapsulated cyanine IR-780 increased cellular oxidative stress. We observed an increase of MDA concentration as a marker of lipid peroxidation and a decrease of free thiol groups as an effect of protein oxidation. Some data showed that both of the two main constituents of cellular membrane, i.e., lipids and protein, may be damaged by the photodynamic reaction (3,49,50). The distinct photodynamic effect was observed generally 3 h after exposure of the treated cells to light (Fig. 8). The increase of time of incubation after irradiation does not lead to any changes in level of oxidative stress markers under the experimental conditions. The loaded cyanine PBCA nanocapsules and free cyanine significantly increased lipid peroxidation in the breast cancer cells after 3 h of irradiation in comparison to control untreated cells or cells incubated with photosensitizer without light excitation.

The relative increase of the lipid peroxidation product (MDA) as well as the most significant effect of oxidation of protein thiol groups were observed after MCF-7/WT cell photoirradiation in the presence of nanocapsule 1, while the smallest effect was observed for 4 (Fig. 8). Relatively high values of the MDA concentration, determined for cells in the case of system 4 (Fig. 7A) were caused by higher amounts of cells in the experimental samples. However, it should be underlined that the MDA increase after irradiation was the lowest among the studied systems. The decrease of oxidative stress markers investigated in MCF-7/WT cells treated with nanocapsules with IR-780 after a long time of storage confirmed the results of the FACS and CLSM observations (Table IV). It is evident that nanocapsule system 1 (according to Table II) showed better time-dependent stability in comparison to system 2, which was observed in photodynamic effects and changes in oxidative stress markers.

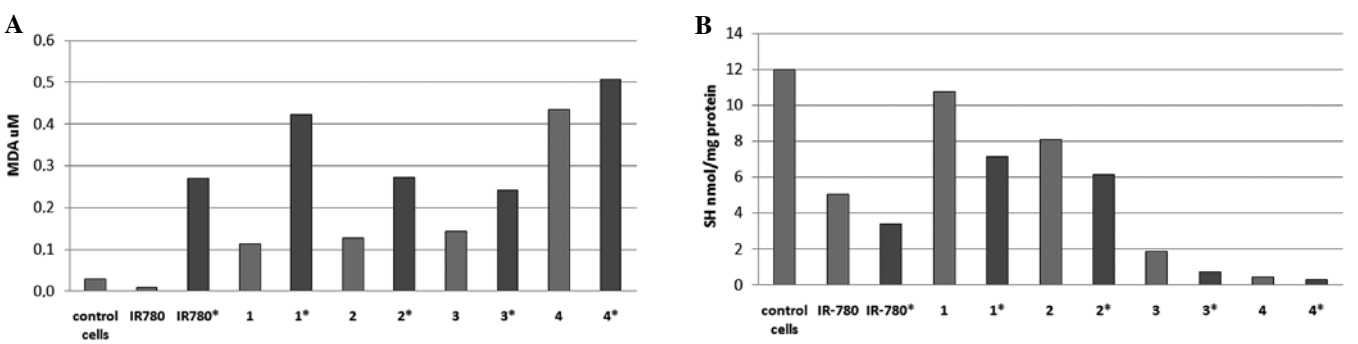

Figure 8. Stress marker determination after photoirradiation of MCF-7/WT cells treated with various PBCA nanocapsules: (A) MDA concentration changes during lipid peroxidation, (B) level of free-SH group during protein oxidation. Asterisk indicated samples which were irradiated for 3 h before MDA or SH level determination.

Table IV. Influence of nanocapsules storage time upon the photodynamic effect of IR-780 cyanine delivered to the MCF-7/WT cells with PBCA nanocapsules (systems 1 and 2 according to Table II).

Storage time group (weeks)	Nanocapsule system	Cell survival decrease (%)	MDA increase (nM)	Decrease of thiol level in proteins (nanomol/mg of protein)
1	1	15	0.320	1.80
	2	20	0.145	1.32
10	1	10	0.216	0.84
	2	13	0.088	0.55
	1			
15	2	12.5	0.250	0.32
		10	0.028	0.12

[a]Data for 10 μM IR-780 concentration in treated cells.

Our results prove that the cyanine IF-780 delivered in PBCA nanocapsules to the MCF-7/WT cells is still sensitive to photoirradiation. Intensity of oxidative stress generated by the photosensitizer depends on the effective uptake of nanocapsules by the treated cells. Probably those effects are dependent on the type of surfactant structure used to form all the studied templates applied in nanocapsule fabrication. The delivery system based on C12DGHA constitutes the most stabile and promising nanocarrier for delivering IR-780 to cancer cells, and that confirms their potential usefulness for PDT.

In conclusion our present findings recommend the PBCA nanocapsules based on o/w microemulsions stabilized by non-ionic aldonamide-type surfactants as a convenient carrier for the hydrophobic cyanine IR-780. General features of the performed experiments reveal that biological responses of breast cancer cells treated by poly(*n*-butyl cyanoacrylate) nanocapsules are dependent on the surfactant structure. The obtained polymeric nanocarriers loaded with IR-780 prepared by interfacial polymerization can be applied as efficient photosensitizer carriers for photodynamic therapy due to biocompatibility. It is worth emphasizing that cyanine delivered to the cells maintains active monomolecular form and is regularly distributed in the cytoplasm of cancer MCF-7/WT cells. The irradiation of cyanine IR-780 release from nanocapsules in the MCF-7/WT cells generated a photodynamic effect and increased oxidative stress.

Acknowledgements

This work was supported by Wrocław University of Technology [research related to C12DHA and bis(C12GHA)], Poland and Wroclaw Research Center EIT$^+$ under the project 'Biotechnologies and advanced medical technologies' - BioMed (POIG 01.01.02-02-003/08-00) financed from the European Regional Development Fund Operational Programme Innovative Economy and the Polish Ministry of Science and Higher Education (grant no. N205013854) [research related to C12DGA and bis(C12GA)].

References

1. Celli JP, Spring BQ, Rizvi I, Evans CL, Samokoe KS, Verma S, Pogue BW and Hasan T: Imaging and photodynamic therapy: mechanism, monitoring, and optimization. Chem Rev 110: 2795-2838, 2010.
2. Allison RR, Bagnato VS, Cuenca R, Dovnie GH and Sibata CH: The future of photodynamic therapy in oncology. Future Oncol 2: 53-71, 2006.
3. Saczko J, Kulbacka J, Chwiłkowska A, Ługowski M and Banaś T: Levels of lipid peroxidation in A549 cells after PDT in vitro. Proc Ann Acad Med Bialostoc 49: 82-84, 2004.
4. Castano AP, Demidova TN and Hamblin MR: Mechanisms in photodynamic therapy: part two - cellular, cell metabolism and modes of cell death. Photodiag Photodyn Ther 2: 1-23, 2005.
5. Oleinick NL, Morris RL and Belichenko I: The role of apoptosis in response to photodynamic therapy: what, where, why, and how. Photochem Phtobiol Sci 1: 1-21, 2002.
6. Castano AP, Demidova TN and Hamblin MR: Mechanisms in photodynamic therapy: part one - photosensitizers, photochemistry and cellular localization. Photodiagn Photodyn Ther 1: 279-293, 2004.
7. Kassab K: Photophysical and photosensitizing properties of selected cyanines. J Photochem Photobiol B 68: 15-22, 2002.
8. Kulbacka J, Pola A, Mosiadz D, Choromanska A, Nowak P, Kotulska M, Majkowski M, Hryniewicz-Jankowska A, Purzyc L and Saczko J: Cyanines as efficient photosensitizers in photodynamic reaction: photophysical properties and in vitro photodynamic activity. Biochemistry (Moscow) 76: 473-479, 2011.
9. Santos PF, Reis LV, Almeida P, Oliviera AS and Vieira Ferreira LF: Singlet oxygen generation ability of squarylium cyanine dyes. J Photochem Photobiol A 160: 159-161, 2003.
10. Nowak-Sliwinska P, Karocki A, Elas M, Pawlak A and Stochel G: Verteporfin, photofrin II, and merocyanine 540 as PDT photosensitizers against melanoma cells. Biochem Biophys Res Commun 349: 549-555, 2006.
11. Breunig M, Bauer S and Goepferich A: Polymers and nanoparticles: intelligent tools for intracellular targeting. Eur J Pharm Biopharm 68: 112-128, 2008.
12. Cho K, Wang X, Nie S, Chen ZG and Shin DM: Therapeutic nanoparticles for drug delivery in cancer. Clin Cancer Res 14: 1310-1316, 2008.
13. Torchilin VP: Targeted pharmaceutical nanocarriers for cancer therapy and imaging. AAPS J 9: 128-147, 2007.
14. Guterres SS, Alves MP and Pohlmann AR: Polymeric nanoparticles, nanospheres and nanocapsules, for cutaneous applications. Drug Target Insights 2: 147-157, 2007.
15. Johnston APR, Cortez C, Angelatos AS and Caruso F: Layer-by-layer engineered capsules and their applications. Curr Opin Colloid Interface Sci 11: 203-209, 2006.

16. Vauthier C, Dubernet C, Fattal E, Pinto-Alphandary H and Couvreur P: Poly(alkylcyanoacrylates) as biodegradable materials for biomedical applications. Adv Drug Deliv Rev 55: 519-548, 2003.
17. Pietkiewicz J, Zielińska K, Saczko J, Kulbacka J, Majkowski M and Wilk KA: New approach to hydrophobic cyanine-type photosensitizer delivery using polymeric oil-cored nanocarriers: hemolytic activity, in vitro cytotoxicity and localization in cancer cells. Eur J Pharm Sci 39: 322-335, 2010.
18. Lambert G, Fattal E, Pinto-Alphandary H, Gulik A and Couvreurr P: Polyisobutylcyanoacrylate nanocapsules containing an aqueous core as a novel colloidal carrier for delivery of oligonucleotides. Pharm Res 17: 707-714, 2000.
19. Li YP, Pei YY, Zhou ZH, Zhang XY, Gu ZH, Ding J, Zhou JJ, Gao XJ and Zhu JH: Stealth polycyanoacrylate nanoparticles as tumor necrosis factor-carriers: pharmacokinetics and anti-tumor effects. Biol Pharm Bull 24: 662-665, 2001.
20. Graf A, Ablinger E, Peters S, Zimmer A, Hook S and Rades T: Microemulsions containing lecithin and sugar-based surfactants: nanoparticle templates for delivery of proteins and peptides. Int J Pharm 350: 351-360, 2008.
21. Graf A, Rades T and Hook SM: Oral insulin delivery using nanoparticles based on microemulsions with different structure-types: optimization and in vivo evaluation. Eur J Pharm Sci 37: 53-61, 2009.
22. Wilk KA, Zielińska K, Pietkiewicz J and Saczko J: Loaded nanoparticles with cyanine-type photosensitizers: preparation, characterization and encapsulation. Chem Eng Trans 17: 987-992, 2009.
23. Wilk KA, Syper L, Burczyk B, Sokołowski A and Domagalska BW: Synthesis and surface properties of new dicephalic saccharide-derived surfactants. J Surfact Det 3: 185-192, 2000.
24. Komorek U and Wilk KA: Surface and micellar properties of new non-ionic gemini aldonamide-type surfactants. J Colloid Interface Sci 271: 206-211, 2004.
25. Wilk KA, Laska U, Zielińska K and Olszowski A: Fluorescence probe studies upon microenvironment characteristics and aggregation properties of gemini sugar surfactants in an aquatic environment. J Photochem Photobiol A 219: 204-210, 2011.
26. Wilk KA, Syper L, Domagalska BW, Komorek U, Maliszewska I and Gancarz R: Aldonamide-type gemini surfactants: synthesis, structural analysis and biological properties. J Surfact Det 5: 235-244, 2002.
27. Wilk KA, Zielińska K, Hamerska-Dudra A and Jezierski A: Biocompatible microemulsions of dicephalic aldonamide-type surfactants: formulation, structure and temperature influence. J Colloid Interface Sci 334: 87-95, 2009.
28. Delaey E, van Laar F, De Vos D, Kamuhabwa A, Jacobs P and De Witte PA: Comparative study of the photosensitizing characteristics of some cyanine dyes. J Photochem Photobiol B 55: 27-36, 2000.
29. Saczko J, Skrzypek W, Chwiłkowska A, Choromańska A, Poła A, Gamian A and Kulbacka J: Photo-oxidative action in cervix carcinoma cells induced by HpD-mediated photodynamic therapy. Exp Oncol 31: 195-199, 2009.
30. Ying X, Wen H, Lu WL, Du J, Guo J, Tian W, Men Y, *et al*: Dual-targeting daunorubicin liposomes improve the therapeutic efficacy of brain glioma in animals. J Control Release 141: 183-192, 2010.
31. Da Silva AR, Inada NM, Rettori D, Baratti MO, Vercesi AE and Jorge RA: In vitro photodynamic activity of chloro (5,10,15,20-tetraphenylporphyrinato) indium(III) loaded-poly (lactide-co-glycolide) nanoparticles in LNCaP prostate tumour cells. J Photochem Photobiol B 94: 101-112, 2009.
32. Kulbacka J, Bar J, Chwilkowska A, Dumanska M, Drag-Zalesinska M, Wysocka T, Stach K, *et al*: Oxidative modulation of marcaine and lekoptin in H9C2 rat myoblasts. Acta Pharmacol Sin 30: 184-192, 2009.
33. Subramanian N, Ghosal SK, Acharya A and Moulik SP: Formulation and physicochemical characterization of microemulsion system using iso-propyl myristate, medium-chain glyceride, polysorbate 80 and water. Chem Pharm Bull 53: 1530-1535, 2005.
34. Wilson BC and Patterson MS: The physics, biophysics and technology of photodynamic therapy. Phys Med Biol 5: 61-109, 2008.
35. Castano AP, Mroz P and Hamblin MR: Photodynamic therapy and anti-tumour immunity. Nat Rev Cancer 6: 535-545, 2006.
36. Wilk KA, Zielinska K, Jarzycka A and Pietkiewicz J: Human erythrocyte hemolysis induced by bioinspired sugar surfactants. Progr Colloid Polym Sci 138: 189-192, 2011.
37. Zielinska K, Pietkiewicz J, Saczko J and Wilk KA: Microemulsion stabilized by gemini, dicephalic and single-head single tail sugar surfactants as biologically important systems: hemolytic activity and cytotoxic studies. Progr Colloid Polym Sci 138: 193-196 2011.
38. Müller RH, Jacobs C and Kayser O: Nanosuspensions as particulate drug formulations in therapy. Rationale for development and what we can expect for the future. Adv Drug Deliv Rev 47: 3-19, 2001.
39. Haillaireau H and Couvreur P: Nanocarriers' entry into the cell: relevance to drug delivery. Cell Mol Life Sci 66: 2873-2896, 2009.
40. Panyam J, Sahoo SK, Prabha S, Bargar T, Labhasetwar V: Fluorescence and electron microscopy probes for cellular and tissue uptake of poly(D,L-lactide-co-glycolide) nanoparticles. Int J Pharm 262: 1-11, 2003.
41. Win KY and Feng SS: Effects of particle size and surface coating on cellular uptake of polymeric nanoparticles for oral delivery of anticancer drugs. Biomaterials 26: 2713-2722, 2005.
42. Yordanov G, Abrashev N and Dushkin C: Poly(n-butylcyanoacrylate) submicron particles loaded with ciprofloxacin for potential treatment of bacterial infections. Progr Colloid Polym Sci 137: 53-59, 2010.
43. Han A, Yang L and Frazier AB: Quantification of the heterogeneity in breast cancer cell lines using whole-cell impedance spectroscopy. Clin Cancer Res 13: 139-143, 2007.
44. Konemann S, Schuck A, Malath J, Rupek T, Horn K, Baumann M, Vormoor J, *et al*: Cell heterogeneity and subpopulations in solid tumors characterized by simultaneous immunophenotyping and DNA content analysis. Cytometry 41: 172-177, 2000.
45. Chaudhery V, Lu M, Huang CS, George S and Cunningham BT: Photobleaching on photonic crystal enhanced fluorescence surfaces. J Fluoresc DOI 10.1007/s10895-010-0760-8, 2010.
46. Ai H, Pirk JJ, Shuai X, Boothman DA and Gao J: Interaction between self-assembled polyelectrolyte shells and tumor cells. J Biomed Mater Sci 73: 303-312, 2005.
47. Skřivanová K, Škorpíková J, Švihálek J, Mornstein V and Janich R: Photochemical properties of a potential photosensitiser indocyanine green in vitro. J Photochem Photobiol B 85: 150-154, 2006.
48. Konan YN, Gurny R and Allemann E: State of the art in the delivery of photosensitizers for photodynamic therapy. J Photochem Photobiol B 66: 89-106, 2002.
49. Zajdel A, Latocha M and Wilczok A: The effect of photodynamic treatment on the levels of aldehydic lipid peroxidation products in human tumor cell. Adv Clin Exp Med 17: 599-605, 2008.
50. Nowis D, Makowski M, Stokłosa M, Legat M, Issat T and Gołąb J: Direct tumor damage mechanisms of photodynamic therapy. Acta Biochim Pol 52: 339-352, 2005.